ELSEVIER

Journal of Alloys and Compounds 408–412 (2006) 945–951

Journal of ALLOYS AND COMPOUNDS

www.elsevier.com/locate/jallcom

Lanthanide complexes of some high energetic compounds (**I**), crystal structures and thermal properties of 3-nitro-1,2,4-triazole-5-one (NTO) complexes

Sock-Sung Yun [a,*], Jae-Kyung Kim [b], Chong-Hyeak Kim [c]

[a] *Department of Chemistry, Chungnam National University, Daejeon 305-764, Republic of Korea*
[b] *High Explosive Team, Agency for Defense Development, P.O. Box 35-5, Daejeon 305-600, Republic of Korea*
[c] *Chemical Analysis Laboratory, Korea Research Institute of Chemical Technology, P.O. Box 107, Daejeon 305-600, Republic of Korea*

Received 30 July 2004; received in revised form 19 November 2004; accepted 30 November 2004
Available online 14 June 2005

Abstract

The title complexes with NTO ligand, $[Pr_2(NTO)_4(H_2O)_{10}]\cdot 2NTO\cdot 6H_2O$, **I**; $[Gd(NTO)_2(H_2O)_6]\cdot NO_3\cdot 2H_2O$, **II**; $[Ho(NTO)_2(H_2O)_6]\cdot NO_3\cdot 2H_2O$, **III**, have been synthesized and their crystal structures analyzed by X-ray diffraction methods. Complex **I** crystallized in the monoclinic *Pc* space group; **II**, triclinic $P\bar{1}$; **III,** monoclinic $P2_1/n$. In complex **I**, the Pr(III) atoms have two different coordination numbers. Ten coordinated Pr(1) atom forms two five-membered chelate rings by combining two NTO ligands bridged to Pr(2) atom. Eight coordinated Pr(2) atom has two terminal NTO ligands and two NTO ligands bridged to Pr(1) atom. Bridging of NTO ligands between Pr(1) and Pr(2), give a novel infinite one-dimensional coordination polymer. There are two free NTO molecules and six crystalline water molecules in the crystal lattice. In iso-structural complexes **II** and **III**, the Gd(III) and Ho(III) atoms have eight coordinated by two carbonyl O atoms of two different NTO rings and six water molecules, respectively. There are one NO_3 ion and two crystalline water molecules in the crystal lattice. The crystal structures are stabilized by three-dimensional network of the intermolecular $N{-}H\cdots O_{Nitrate}$ and $N{-}H\cdots N_{NTO}$ hydrogen bonds. Based on the results of TG-DTG thermal analysis, the thermal decomposition reaction of complex **I** was analyzed to have three distinctive stages such as the dehydration of water, the cleavage of NTO ring and the formation of metal oxide, while complexes **II** and **III** were proceeded through four stages including the decomposition of NO_3 ion.

Keywords: Lanthanide complex; 3-Nitro-1,2,4-triazole-5-one (NTO); Crystal structure; Thermal analysis

1. Introduction

The strategy for the development of new energetic materials is based on the requirements such as high energy density, insensitivity to mechanical insults, resistance to chemical composition, and the ability to be formulated with other materials for fabrication into practical devices. 3-Nitro-1,2,4-triazol-5-one (NTO) has been attracted as a candidate for such high energetic materials. NTO is the high energy explosive which is thermally stable and less sensitive than commonly used nitroamine explosive such as 1,3,5-trinitrohexahydro-*s*-triazine (RDX) and octahydro-1,3,5,7-tetranitro-1,3,5,7-tetrazocine (HMX) [1]. NTO is white crystalline solid, relatively acidic ($pK_a = 3.67$) in aqueous solution, and forms stable complexes with a large number of metal ions [2–9] as well as aromatic and aliphatic amines. The metal complexes of NTO are also interesting novel compounds probably used in ammunition, propellants and energetic catalyst, especially its rare-earth metal salts [2,10–13]. When NTO salts were added to a formula system, their burning velocity and specific impulse are greatly improved, while the index of pressure decreases [14].

As an extension of the NTO complex study, we have investigated the crystal structure, thermal stability and decom-

* Corresponding author. Tel.: +82 42 821 5478; fax: +82 42 822 8632.
E-mail address: ssyun@cnu.ac.kr (S.-S. Yun).

0925-8388/$ – see front matter © 2005 Elsevier B.V. All rights reserved.
doi:10.1016/j.jallcom.2004.11.087

position mechanism of praseodymium-, gadolinium- and holmium-NTO complex as the lighter and heavier lanthanide, respectively. Here we report the preparation, crystal structures and thermal properties of $[Pr_2(NTO)_4(H_2O)_{10}]\cdot 2NTO\cdot 6H_2O$, **I**; $[Gd(NTO)_2(H_2O)_6]\cdot NO_3\cdot 2H_2O$, **II**; $[Ho(NTO)_2(H_2O)_6]\cdot NO_3\cdot 2H_2O$, **III**.

2. Experimental

2.1. Preparation and analysis of the complexes

The praseodymium-, gadolinium- and holmium-NTO complexes were prepared according to the following method. The metal solutions were prepared by dissolving respective lanthanide oxides in dilute nitric acid solution with stirring at 60 °C and the pH of solution was adjusted to about 2 with nitric acid solution. The ligand solution was prepared by dissolving NTO in distilled water with stirring at 60 °C and the pH of solution was adjusted to about 7 with lithium hydroxide solution. The metal solution was added dropwise slowly to the ligand solution and then filtrated through a 0.45 μm plastic membrane in order to remove the small amount of precipitate formed. The final solution was allowed to stand in a refrigerator at 5 °C and the lanthanide–NTO crystals were obtained after a few days. The complex was re-crystallized with distilled water at room temperature for 6 months and crystal of the complex suitable for single crystal X-ray diffraction was obtained.

IR spectra of the complexes were recorded on a Bruker IFS-88 infrared spectrometer using KBr pellets methods. The NTO ligand was assigned by the relevant IR absorption bands [15]. Elemental contents of carbon, hydrogen and nitrogen were determined by a Carlo-Erba MOD-1108 elemental analyzer. The contents of Pr, Gd and Ho were determined by a Jobin-Yvon Ultima-C inductively coupled plasma emission spectrometer. The composition of the crystals were deduced from the elemental analyses; the formula of $[Pr_2(NTO)_4(H_2O)_{10}]\cdot 2NTO\cdot 6H_2O$, **I**; $[Gd(NTO)_2(H_2O)_6]\cdot NO_3\cdot 2H_2O$, **II**; $[Ho(NTO)_2(H_2O)_6]\cdot NO_3\cdot 2H_2O$, **III**, are consistent with the results of single crystal X-ray diffraction analyses. Analytically calculated for $C_{12}H_{38}N_{24}O_{34}Pr_2$, **I**, (%): C, 10.72; H, 2.85; N, 25.01; Pr, 20.96. Found: C, 10.58; H, 2.85; N, 25.04; Pr, 21.24. Analytically calculated for $C_4H_{18}N_9O_{17}Gd$, **II**, (%): C, 7.73; H, 2.92; N, 20.29; Gd, 25.30. Found: C, 7.71; H, 2.67; N, 19.85; Gd, 24.99. Analytically calculated for $C_4H_{18}N_9O_{17}Ho$, **III**, (%): C, 7.64; H, 2.88; N, 20.04; Ho, 26.21. Found: C, 7.96; H, 2.67; N, 19.57; Ho, 26.53. The thermal decomposition of the complexes were investigated on a Mettler-Toledo TGA-50 and Mettler-Toledo DSC-821 thermal analyzer, respectively. The conditions of TG and DSC analysis are as follow. For TG: sample mass, about 1 mg; heating rate, 10 °C/min; atmosphere, nitrogen, and for DSC: sample mass, about 1 mg; heating rate, 10 °C/min; atmosphere, static air; reference sample, indium.

2.2. X-ray crystallography

A single crystal of the title complex was coated with epoxy glue in order to prevent spontaneous liberation of water molecules from the specimen under ambient conditions. The intensity data were collected at room temperature on an Siemens P4 four-circle X-ray diffractometer with graphite-monochromated Mo Kα radiation (λ = 0.71073 Å). Three standard reflections were monitored every 97 reflections; no remarkable decays were observed through data collection. Lorentz and polarization corrections were applied to the intensity data, and a semi-empirical absorption correction based on the psi-scans was applied [16].

All calculations in the structural solution and refinement were performed using the Siemens SHELXTL crystallographic software package [17]. The structure was solved by the heavy atom method [18] and refined by successive full-matrix least-squares method followed by difference Fourier maps. All the non-hydrogen atoms were refined anisotropically; all the hydrogen atoms were put into calculated positions with the isotropic thermal parameters. Further details of the crystallographic and experimental data for complexes **I**, **II** and **III** are given in Table 1.

3. Results and discussion

3.1. Crystal structure of $[Pr_2(NTO)_4(H_2O)_{10}]\cdot 2NTO\cdot 6H_2O$, *I*

Molecular structure and perspective view of complex **I**, are illustrated in Figs. 1 and 2, respectively. Selected bond distances and angles are listed in Table 2.

Fig. 1 shows that the important structural feature of the complex **I** is the presence of the bridged ligands and the terminal ligands in the bimetallic structure. The terminal NTO ligand behaves as a monodentate ligand, while bridged NTO ligand behaves as a tridentate ligand. The central Pr(III) atoms have two different coordinate numbers; Pr(1) has ten coordination numbers and its coordination polyhedron forms distorted bicapped square antiprism, while Pr(2) has eight coordination and forms dodecahedron. The Pr(1) atom is directly coordinated to six water molecules and forms two chelate rings by combining two different NTO ligands bridged to Pr(2) atom. Each five-membered chelate ring is formed by interacting the Pr(1) atom with N atom in the NTO ring and O atom of nitro group on the same side of the NTO ligand. The chelated NTO ligands are posed to be a trans configuration. On the other hand, the Pr(2) atom is coordinated to four O atoms of water molecules and four carbonyl O atoms from two terminal NTO ligands and two NTO ligands bridged to Pr(1) atom. The carbonyl O atom of bridged NTO ligand is connected to two metal ions, Pr(1) and Pr(2), and give an one-dimensional coordination polymer structure. There are two free NTO molecules and six crystalline water molecules in the crystal lattice.

Table 1
Crystallographic and experimental data for complexes **I**, **II** and **III**

Compound	**I**	**II**	**III**
Chemical formula	$C_{12}H_{38}N_{24}O_{34}Pr_2$	$C_4H_{18}N_9O_{17}Gd$	$C_4H_{18}N_9O_{17}Ho$
Formula weight	1344.48	621.52	629.20
Crystal system	Monoclinic	Triclinic	Monoclinic
Space group	*Pc*	$P\bar{1}$	$P2_1/n$
Unit cell dimensions			
a (Å)	12.043(3)	6.151(1)	6.1396(9)
b (Å)	9.956(1)	11.618(3)	25.864(4)
c (Å)	18.611(3)	25.985(8)	11.597(2)
α (°)	90	90.01(2)	90
β (°)	102.01(1)	90.02(2)	98.23(1)
γ (°)	90	98.07(2)	90
Volume, (Å^3)	2182.6(6)	1838.4(8)	1822.6(5)
Z	2	4	4
Calculated density	2.046	2.246	2.293
Absorption coefficient	2.340	3.718	4.452
F(0 0 0)	1336	1220	1232
θ Range for data collection (°)	2.05–27.50	1.77–27.50	1.94–27.50
Index ranges	$-1 \le h \le 15$, $-1 \le k \le 12$, $-24 \le l \le 23$	$-7 \le h \le 1$, $-15 \le k \le 15$, $-1 \le l \le 33$	$-7 \le h \le 1$, $-1 \le k \le 33$, $-15 \le l \le 15$
Reflections collected/unique	5904/5380 (R_{int} = 0.0349)	5224/5096 (R_{int} = 0.0442)	4711/3735 (R_{int} = 0.1283)
Data/restraints/parameters	5380/2/649	5096/0/559	3735/0/281
Goodness-of-fit on F^2	1.080	1.287	1.082
Final *R* indices [$I > 2\sigma(I)$]	0.0399, 0.1038	0.0544, 0.1480	0.0885, 0.2219

The bond distances of Pr–O coordination bonds are observed in range from 2.366(5) to 2.971(6) Å. The average Pr–O_{water} and Pr–N_{NTO} bond distances are 2.495(6) and 2.695(6) Å, respectively. Some remarkable features have been observed that bond distances of the bridged ligands are considerably longer than those of the terminal ligands as listed in Table 2; Pr(1)–O(13) 2.958(5), Pr(1)–O(22) 2.971(6), Pr(2)–O(31) 2.395(6), Pr(2)–O(41) 2.366(5) Å. This means that coordination bond strength of the bridged ligand is significantly weak. On the other hand, there is no metal–metal interaction since the distance of Pr(1)–Pr(2) atoms is 6.20 Å. The bond distances and angles related to NTO ligand are not unusual and good agreement with the calculated ones by Ritchie [19] and by others [20].

As shown in Fig. 2, the crystal structure of complex **I** give a novel infinite zig-zag one-dimensional coordination polymer. The formation of one-dimensional coordination polymer is unusual compared with zero-dimensional structure of $H[Pr(NTO)_4(H_2O)_4]\cdot 2H_2O$ [13]. There are many inter-molecular hydrogen bonds between the N–H moieties of NTO ligand and water molecules, the O and N

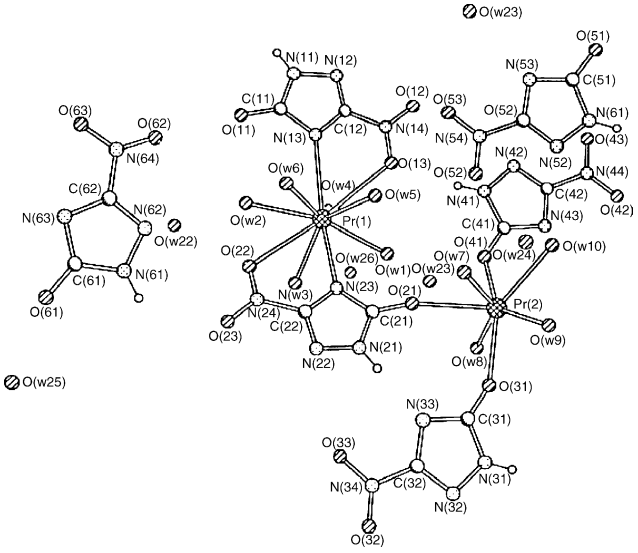

Fig. 1. Molecular structure of $[Pr_2(NTO)_4(H_2O)_{10}]\cdot 2NTO\cdot 6H_2O$, **I**.

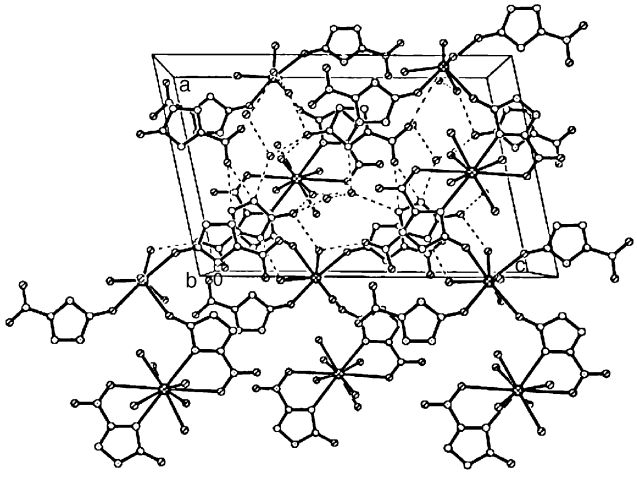

Fig. 2. Perspective view of $[Pr_2(NTO)_4(H_2O)_{10}]\cdot 2NTO\cdot 6H_2O$, **I**.

Table 2
Selected bond lengths (Å) and angles (°) for complex **I**

Pr(1)—O(w1)	2.494(7)
Pr(1)—O(w3)	2.471(6)
Pr(1)—O(w5)	2.512(6)
Pr(1)—N(13)	2.694(6)
Pr(1)—O(22)	2.971(6)
Pr(2)—O(w7)	2.491(6)
Pr(2)—O(w9)	2.519(6)
Pr(2)—O(21)	2.495(5)
Pr(2)—O(41)	2.366(5)
Pr(1)—O(w2)	2.478(7)
Pr(1)—O(w4)	2.502(6)
Pr(1)—O(w6)	2.446(7)
Pr(1)—O(13)	2.958(5)
Pr(1)—N(23)	2.697(6)
Pr(2)—O(w8)	2.517(5)
Pr(2)—O(w10)	2.521(5)
Pr(2)—O(31)	2.395(6)
Pr(2)—O(11)[a]	2.428(6)
O(13)—Pr(1)—N(13)	55.6(2)
O(13)—Pr(1)—N(23)	118.9(2)
N(13)—Pr(1)—N(23)	152.3(1)
O(31)—Pr(2)—O(41)	143.8(2)
O(31)—Pr(2)—O(11)[a]	82.6(2)
O(41)—Pr(2)—O(11)[a]	92.3(2)
O(13)—Pr(1)—O(22)	165.0(2)
N(13)—Pr(1)—O(22)	120.3(2)
O(22)—Pr(1)—N(23)	56.7(2)
O(31)—Pr(2)—O(21)	88.4(2)
O(41)—Pr(2)—O(21)	76.4(2)
O(21)—Pr(2)—O(11)[a]	146.5(2)

[a]Symmetry transformations used to generate equivalent atoms: $-x+1/2$, $y-1/2$, $-z-1/2$.

atoms of NTO ligand: N(11)–H(11)···N(43) 2.832(9) Å, 167.2°; N(21)–H(21)···N(33) 2.844(9) Å, 169.5°; N(31)–H(31)···O(22) 3.153(9) Å, 173.0°; N(41)–H(41)···O(13) 3.012(9) Å, 170.8°; N(51)–H(51)···O(63) 2.75(1) Å, 124.2°; N(51)–H(51)···O(w7) 3.125(8) Å, 124.8°; N(61)–H(61)···O(w26) 2.903(9) Å, 162.0°. These hydrogen bond interactions seem to contribute to stabilization of the crystal structure.

3.2. Crystal structures of $[Gd(NTO)_2(H_2O)_6]\cdot NO_3\cdot 2H_2O$, **II**, and $[Ho(NTO)_2(H_2O)_6]\cdot NO_3\cdot 2H_2O$, **III**

The common structural feature observed for complexes **II** and **III** are iso-structural with each other. Molecular structure and perspective view of complex **III**, are illustrated in Figs. 3 and 4, respectively. Selected bond distances and angles for complexes **II** and **III** are listed in Table 3.

As shown in Fig. 3, the central Ho(III) atom has eight coordinate numbers and its coordination polyhedron forms square antiprism. The Ho(1) atom is coordinated by six O atoms of water molecules and two carbonyl O atoms of two terminal NTO ligands. There are one NO_3 ions and two water molecules of crystallization in the crystal lattice. The NO_3 ions may come from dilute nitric acid, which was used to

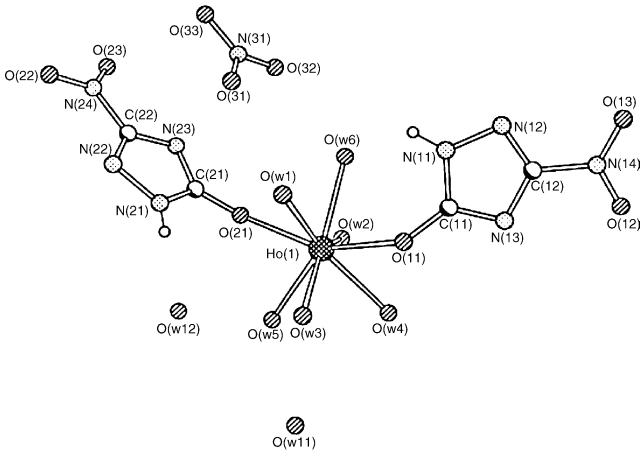

Fig. 3. Molecular structure of $[Ho(NTO)_2(H_2O)_6]\cdot NO_3\cdot 2H_2O$, **III**.

dissolve the holmium oxide. We can notice a similar case of $[Y(NTO)_2(NO_3)(H_2O)_5]\cdot 2H_2O$ published by Song et al. [5]. However, the coordination behaviors of free NO_3 ion in our crystal structure differs from theirs, where the NO_3 ions directly coordinated to the central Y(III) atom. As listed in Table 3, the bond distances of Ho–O coordination bonds are observed in range from 2.280(7) to 2.505(7) Å. The average Ho–O_{water} and Ho–O_{NTO} bond distances are 2.395(7) and 2.286(6) Å, respectively.

As shown in Fig. 4, the crystal structure of complex **III** give a zero-dimensional coordination compound. There are inter-molecular hydrogen bonds between the N–H moieties of NTO ligand and the N atom of NTO ligand and the O atom of NO_3 ion: N(11)–H(11)···N(22) 2.91(1) Å, 146.1°; N(21)–H(21)···O(33) 2.86(1) Å, 167.3°; N(21)–H(21)···O(32) 3.24(1) Å, 133.6°; N(21)–H(21)···N(31) 3.49(1) Å, 160.6°. These hydrogen bond interactions seem to contribute to stabilization of the crystal structure.

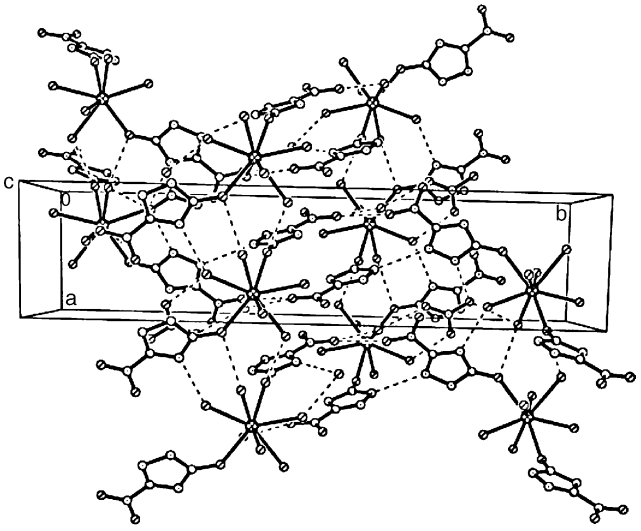

Fig. 4. Perspective view of $[Ho(NTO)_2(H_2O)_6]\cdot NO_3\cdot 2H_2O$, **III**.

Table 3
Selected bond lengths (Å) and angles (°) for complexes **II** and **III**

Gd(1)—O(w1)	2.53(1)
Gd(1)—O(w3)	2.38(1)
Gd(1)—O(w5)	2.424(7)
Gd(1)—O(11)	2.319(7)
Gd(2)—O(w7)	2.414(8)
Gd(2)—O(w9)	2.45(1)
Gd(2)—O(w11)	2.429(8)
Gd(2)—O(31)	2.31(1)
Gd(1)—O(w2)	2.40(1)
Gd(1)—O(w4)	2.441(7)
Gd(1)—O(w6)	2.429(7)
Gd(1)—O(21)	2.327(8)
Gd(2)—O(w8)	2.381(8)
Gd(2)—O(w10)	2.541(7)
Gd(2)—O(w12)	2.425(8)
Gd(2)—O(41)	2.33(1)
Gd(1)—O(11)—C(11)	137.8(8)
O(11)—Gd(1)—O(21)	151.5(3)
Gd(2)—O(41)—C(41)	140.4(9)
Gd(1)—O(21)—C(21)	141.1(7)
Gd(2)—O(31)—C(31)	138.5(8)
O(31)—Gd(2)—O(41)	151.4(3)
Ho(1)—O(w1)	2.360(7)
Ho(1)—O(w3)	2.358(8)
Ho(1)—O(w5)	2.381(7)
Ho(1)—O(11)	2.293(6)
Ho(1)—O(w2)	2.505(7)
Ho(1)—O(w4)	2.402(7)
Ho(1)—O(w6)	2.364(8)
Ho(1)—O(21)	2.280(7)
Ho(1)—O(11)—C(11)	139.5(6)
O(11)—Ho(1)—O(21)	151.6(2)
Ho(1)—O(21)—C(21)	138.7(5)

3.3. Thermal analysis of $[Pr_2(NTO)_4(H_2O)_{10}]\cdot 2NTO\cdot 6H_2O$, **I**

The thermograms of TG-DTG and DSC of the complex **I** were obtained under the conditions of linear temperature increase. As shown in Fig. 5, the thermal decomposition reaction of the complex **I** would proceeds through three stages under our experimental condition: the dehydration of water molecule, the ring cleavage of NTO ligand and the formation of metal oxide. Our results concur with decomposition patterns reported by Xie et al. in their studies with Pr-, Nd- and Sm-NTO complexes [21].

The DSC curve appears to indicate that dehydration process is composed of three steps, but we have to overcome difficulties in distinguishing those clearly from TG-DTG curves because of the crystalline properties of sample. The first step of dehydration is the loss of six crystalline water molecules in the temperature range of 30–61 °C. The mass loss of 8.0% exactly matches with the theoretical calculation for the loss of six water molecules from complex **I**, $[Pr_2(NTO)_4(H_2O)_{10}]\cdot 2NTO\cdot 6H_2O$. The second step occurs from 61 to 121 °C with the peak maximum temperature of 78 °C. The mass loss from the TG-DTG curves is 10.6%, which is also in excellent agreement with the calculated value of 10.7% for the loss of eight coordinated water molecules from $[Pr_2(NTO)_4(H_2O)_{10}]\cdot 2NTO$. The last dehydration step begins at 121 °C and ends at 181 °C. The mass loss for this step is 2.7%. We believe that this results from the loss of two coordinated water molecules from the $[Pr_2(NTO)_4(H_2O)_2]\cdot 2NTO$.

The ring cleavage of NTO ligand occurs from 181 to 352 °C. After the ring cleavage of NTO ligand, the characteristic IR absorption bands of the –C–NO_2 group at 1515 and 1302 cm^{-1} disappears and new absorption bands of $Pr(OCN)_3$, $Pr_2(CO_3)_3$ and polymers containing the –CO–NH– group come out at 2336, 2178 and 1185, 1506 and 787, and 3342, 1634 and 1378 cm^{-1}, respectively. These observations show that the decomposition residue after this stage are proposed to be mixtures of $Pr(OCN)_3$, $Pr_2(CO_3)_3$ and polymer materials. The amount of each component cannot be analyzed from the results of thermal analysis and it is impossible to calculate the decomposition change stoichiometrically.

The final stage is the metal oxide formation of Pr_6O_{11} in the temperature range of 352–593 °C. The mass loss of this stage is 24.6%. The IR absorption band of 561 cm^{-1} indicates that the metal oxide is formed.

The total mass loss of three decomposition stages is 75.2%, which is in excellent agreement with the calculated value of 75.4%. The mass percentage of metal oxide is 24.8% and mass fraction of Pr in the metal oxide is 21.20%. These values also concur with the mass fraction of Pr in single crystal of complex **I**.

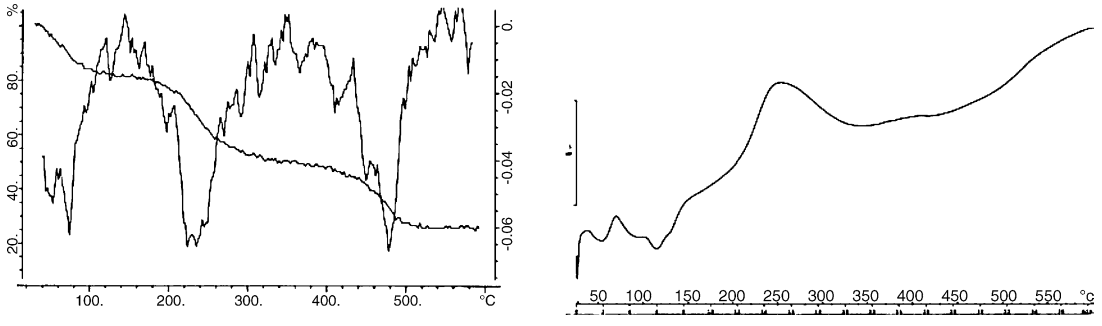

Fig. 5. TG-DTG and DSC curves for $[Pr_2(NTO)_4(H_2O)_{10}]\cdot 2NTO\cdot 6H_2O$, **I**.

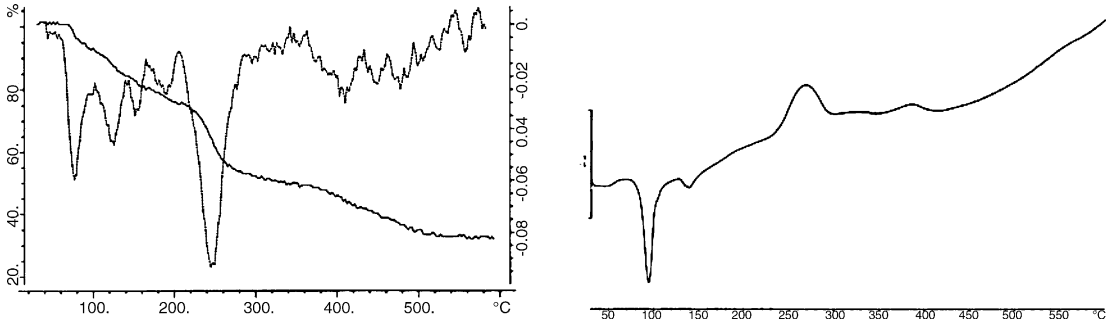

Fig. 6. TG-DTG and DSC curves for $[Ho(NTO)_2(H_2O)_6]\cdot NO_3\cdot 2H_2O$, **III**.

*3.4. Thermal analyses of $[Gd(NTO)_2(H_2O)_6]\cdot NO_3\cdot 2H_2O$, **II**, and $[Ho(NTO)_2(H_2O)_6]\cdot NO_3\cdot 2H_2O$, **III***

The thermograms of TG-DTG and DSC of the complexes **II** and **III** were obtained under the conditions of linear temperature increase. The results of thermal analysis study for $[Gd(NTO)_2(H_2O)_6]\cdot NO_3\cdot 2H_2O$, **II**, and $[Ho(NTO)_2(H_2O)_6]\cdot NO_3\cdot 2H_2O$, **III**, are similar each other in the patterns of TG-DTG and DSC curves. The TG-DTG and DSC curves of the complex **III** are shown in Fig. 6. The thermal decomposition reaction of the complex **III** would proceeds through four stages under our experimental condition: the dehydration of water molecule, the ring cleavage of NTO ligand, the decomposition of NO_3 ion and the formation of metal oxide.

The DSC curve appears to indicate that dehydration process is composed of three steps. The three dehydration stages occur in the temperature range of 30–186 °C. The total mass loss for these three dehydration steps is 22.5% due to the mass loss of two crystalline and six coordinated water molecules.

The ring cleavage of NTO ligand occurs from 186 to 322 °C in TG-DTG curves. The observed mass loss for this stage is 27.6%, which is in excellent accord with the theoretical value of 26.7%. At the end of the NTO ring cleavage, as shown in the Pr-NTO complex, the characteristic IR absorption bands of the –C–NO_2 group at 1516 and 1302 cm^{-1} disappear and new absorption bands of the –CO–NH– group come out at 2340, 1652, 2200 and 1506 cm^{-1}.

The third stage would be the NO_3 ion decomposition stage of the intermediate and occur in the temperature range of 322–427 °C. The mass loss of 9.6% at this stage is good agreement with the calculated value of 9.8%. At the end of this stage, the characteristic IR absorption peak of NO_3 at 1384 cm^{-1} has disappeared and the characteristic absorption peak of $Ho_2(CO_3)_3$ at 1494 and 863 cm^{-1} also appeared.

The final stage would be the metal oxide formation of Ho_2O_3 from the $Ho_2(CO_3)_3$ in the temperature range of 427–592 °C. The observed mass loss of 9.8% also agrees with the calculated value 10.5%.

Total mass loss of the four decomposition stages is 69.5%, which is in good agreement with the calculated value of 69.8%.

4. Supplementary material

Complete lists with atomic coordinates, anisotropic displacement parameters, bond lengths and angles have been deposited at the Cambridge Crystallographic Data Center, 912 Union Road, Cambridge CB2 1EZ, UK [CCDC 246141 for Pr complex, CCDC 246142 for Gd complex and CCDC 246143 for Ho complex].

Acknowledgement

This work was supported by a grant no. R01-2001-00055 from Korea Science and Engineering Foundation.

References

[1] K.Y. Lee, L.B. Chapman, M.D. Coburn, J. Energy Mater. 5 (1987) 27.
[2] R. Hu, J. Song, F. Li, B. Kang, Y. Kuong, Z. Mao, Z. Zhou, Z. Hong, Thermochim. Acta 299 (1997) 87.
[3] J. Song, R. Hu, B. Kang, F. Li, Thermochim. Acta 331 (1999) 49.
[4] J. Song, R. Hu, B. Kang, Y. Lei, F. Li, K. Yu, J. Therm. Anal. Calorim. 55 (1999) 797.
[5] J. Song, B. Ning, R. Hu, B. Kang, Thermochim. Acta 352–353 (2000) 111.
[6] H. Ma, J. Song, X. Sun, R. Hu, S. Gao, K. Yu, Thermochim. Acta 389 (2002) 43.
[7] S. Gao, M. Hu, S. Xia, T. Yue, K. Yu, J. Mol. Struct. 644 (2003) 181.
[8] J. Song, H. Jie, H. Ma, R. Hu, Thermochim. Acta 416 (2004) 39.
[9] J. Song, H. Ma, J. Huang, R. Hu, Thermochim. Acta 416 (2004) 43.
[10] J. Song, R. Hu, F. Li, Chin. Sci. Bull. 41 (1996) 1806.
[11] J. Song, W. Dong, R. Hu, J. Rare Earths 15 (1997) 62.
[12] J. Song, Z. Chen, H. Xiao, R. Hu, F. Li, Acta Chim. Sinica 56 (1998) 270.
[13] J. Song, R. Hu, B. Kang, F. Li, Thermochim. Acta 335 (1999) 19.
[14] S.W. Li, J.M. Wang, X.Y. Fu, J.H. Zhou, Energetic Mater. 1 (1993) 22.

[15] K. Nakamoto, Infrared and Raman Spectra of Inorganic and Coordination Compounds, Part B, Wiley, New York, 1997.
[16] Siemens, XSCANS Data Collection Software Package, Siemens, Karlsruhe, Germany, 1996.
[17] Siemens, SHELXTL Structure Analysis Software Package, Siemens, Karlsruhe, Germany, 1998.
[18] G.M. Sheldrick, Acta Cryst. A 46 (1990) 467.
[19] J.P. Ritchie, J. Org. Chem. 54 (1989) 3553.
[20] D.C. Sorescu, R.L. Teressa, D.L. Thompson, J. Mol. Struct. 384 (1996) 87.
[21] R. Xie, R. Hu, T. Zhang, F. Li, J. Therm. Anal. 29 (1993) 41.